electrons in the lower energy electronic states of each atom were treated with the frozen-core approximation. We use two systems of 120 (24Sr+24Ge+72O) atoms for $SrGeO_3$ and 144 (48Ge+96O) atoms for GeO_2 in a cubic supercell under periodic boundary conditions. Using the Nos´e-Hoover thermostat technique [13, 14], the equations of motion are solved via an explicit reversible integrator [15] with a time step of Δt = 1.2 fs. To obtain a liquid state of both materials, the same procedure is used. We begin by carrying out an *ab initio* MD simulation for about 5 ps at a temperature of 4000 K starting from the crystalline structure [6, 7]. The temperature is selected to be high enough to make the system reach a completely disordered state without the effects of the initial configuration. Then, we decrease the temperature of the system gradually to a target temperature of 2500 K. The number density is determined from zero-pressure condition. The target temperature we have chosen is rather high in order to observe enough number of atomic-diffusion events to analyze the diffusion mechanism in a statistically meaningful way within a limited amount of simulation time. Note that the temperature dependence of physical quantities is not discussed in this paper, and conclusions derived are independent of the selected temperature. The simulation time 7.2 ps, is long enough to achieve good statistics.

3 Results and discussion

3.1. Diffusion mechanism at ambient pressure

The local structure of crystal GeO_2 and $SrGeO_3$ remain even in liquid state, which means that the covalent bonds between Ge and O atoms are preserved in both liquids. It is, however, unclear how Ge-O bonds are exchanged with the diffusion of atoms in the liquids state while retaining the covalent bonds. To clarify the mechanism of atomic diffusion, we investigate the time evolution of bonding nature by utilizing the population analysis [17, 18]. The bond-overlap populations, which give a semiquantitive estimate of the strength of the covalentlike bonding between atoms, are calculated as a function of time.

In liquid GeO_2, Ge atoms are mainly coordinated to four O atoms and O atoms bridge two adjacent Ge atoms as in the crystalline phase, even though atoms diffuse in the liquid state. We find that in this system non-bridging O atom double bonded to a Ge atom is always involved with atomic diffusion accompanied by Ge-O bond switching as in liquid B_2O_3[5]. A typical example of the generation of non-bridging oxygen is shown in figure 1 where the time evolution of the bondoverlap populations associated with the Ge and O atoms of interest is displayed with snapshots of atomic configuration. In the atomic configuration at 0.18 ps (the bottom panel of figure 1) all Ge and O atoms displayed are fourfold- and twofold-coordinated, respectively, to heteroatoms, i.e., there is no bond defect. As shown in the top panel of figure 1, O_{Ge2-O2} begins to increase at about 0.2 ps, which means that a covalent bond is formed between Ge2 and O2. We can see this new Ge2-O2 bond in the snapshot at 0.27 ps. Due to the formation of the bond, both Ge2 and O2 are overcoordinated. Since the overcoordination is unstable, one of covalent bonds around O2 is broken (in the snapshot at 0.38 ps). Note that Ge1 is coordinated to only three oxygens while Ge2 is still over-coordinated. Finally, the covalent bond between Ge2 and O1 is broken. While fourfold-coordination around Ge2 atom is recovered, O1 is coordinated only one Ge atom (Ge1) as displayed in the snapshot at 0.60 ps. In this way, the non-bridging oxygen is generated.

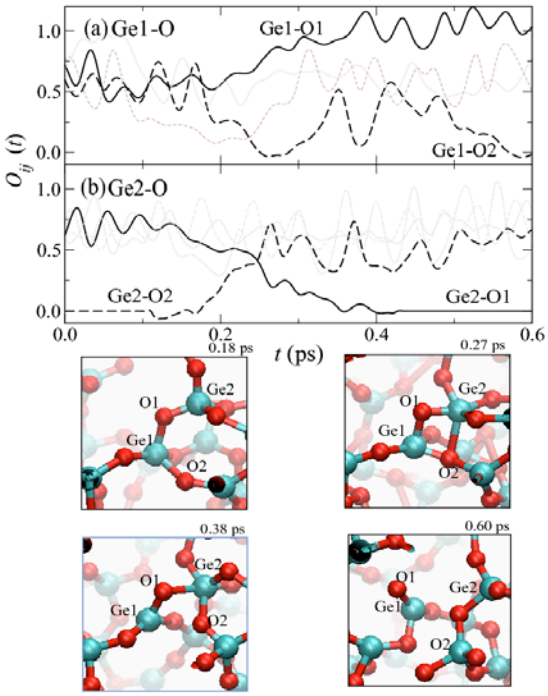

Fig. 1. (Top panel) The time evolution of bond-overlap populations $O_{ij}(t)$ for (a) i = Ge1, $j \in$ O and (b) i = Ge2, $j \in$ O in the process of the formation of a non-bridging oxygen. The thick sold and thick dashed lines show $O_{ij}(t)$ associated with the Ge and O atoms of interest as denoted in the figures. The thin lines show $O_{ij}(t)$ between the Ge atoms of interest (labeled as 'Ge1' and 'Ge2') and their neighboring O atoms except O1 and O2. (Bottom panel) Atomic configurations at t = 0.18, 0.27, 0.38 and 0.60 ps. The large and small spheres show Ge and O atoms, respectively.

In crystalline $SrGeO_3$, all Ge atoms bond to two bridging oxygens and two non-bridging oxygen. This form is also the most stable in the liquid state as in the crystalline states. When Ge-O bond is broken, the local structure is deformed, for example Ge atom might be bonding to three bridging oxyges and only one non-bridging oxygen. A typical example of the bond breaking is shown in figure 2. In the atomic configuration at 0.05 ps, Ge1 bonds to three bridging oxygens and only one non-bridging oxygen. Since this form is not stable, one of bridging oxygen around Ge1 tries to be non-bridging oxygen. As shown in the top panel in figure 2, O_{Ge2-O1} begins to decrease at about 0.15 ps. the covalent bond between Ge2 and O1 is broken, as O_{Ge2-O1} is almost zero for t > 0.35 ps. In the snapshot at 0.35 ps, Ge2 is threefold-coordinated to O atoms, and Ge1 has the most stable form, i.e., bonds to two two bridging oxygens and

two non-bridging oxygens.

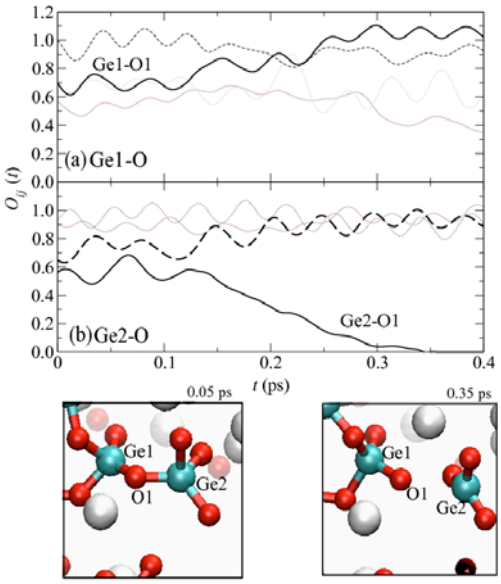

Fig. 2. (Top panel) The time evolution of bond-overlap populations $O_{ij}(t)$ for (a) i = Ge1, $j \in$ O and (b) i = Ge2, $j \in$ O in the process of the formation of a non-bridging oxygen. The thick sold and thick dashed lines show $O_{ij}(t)$ associated with the Ge and O atoms of interest as denoted in the figures. The thin lines show $O_{ij}(t)$ between the Ge atoms of interest (labeled as 'Ge1' and 'Ge2') and their neighboring O atoms except O1. (Bottom panel) Atomic configurations at t = 0.05 and 0.35 ps. The large, middle and small spheres show Sr, Ge and O atoms, respectively.

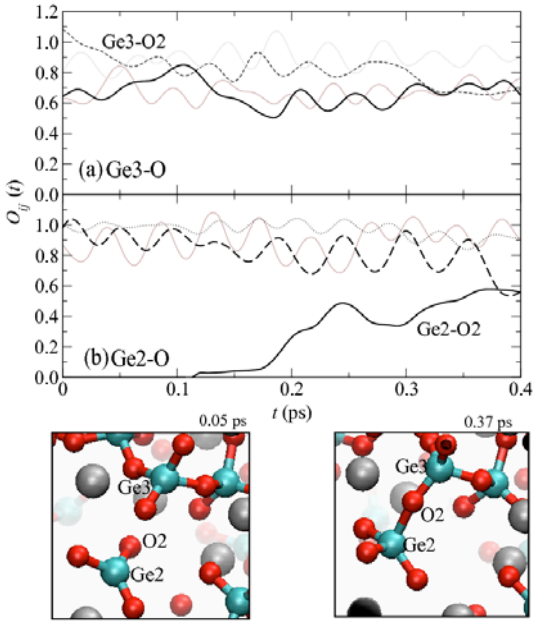

Fig. 3. (Top panel) The time evolution of bond-overlap populations $O_{ij}(t)$ for (a) i = Ge3, $j \in$ O and (b) i = Ge2, $j \in$ O in the process of the formation of a non-bridging oxygen. The thick sold and thick dashed lines show $O_{ij}(t)$ associated with the Ge and O atoms of interest as denoted in the figures. The thin lines show $O_{ij}(t)$ between the Ge atoms of interest (labeled as 'Ge1' and 'Ge2') and their neighboring O atoms except O2. (Bottom panel) Atomic configurations at t = 0.05 and 0.37 ps. The large, middle and small spheres show Sr, Ge and O atoms, respectively.

The disappearance process of threefold-coordinated Ge atom (Ge2) is shown in figure 3. First, the threefold-coordinated Ge2 approaches non-bridging oxygen O2 to form a new covalent bond between them. We see that O_{Ge2-O2} gradually increases for t > 0.12 ps as shown in the top panel of figure 3, which means that the formation of covalent bond between Ge2 and O2 as displayed in the snapshot at 0.37 ps.

3.2 Diffusion mechanism under high pressure

Figure 4 shows the diffusion coefficients D_α for α = Ge and O atoms as a function of pressure. Clearly, only liquid GeO_2 has a diffusion maximum around 5 GPa, while D_α in liquid $SrGeO_3$ decreases monotonically. In liquid GeO_2, the atomic diffusion with concerted reaction appears when pressure increases.

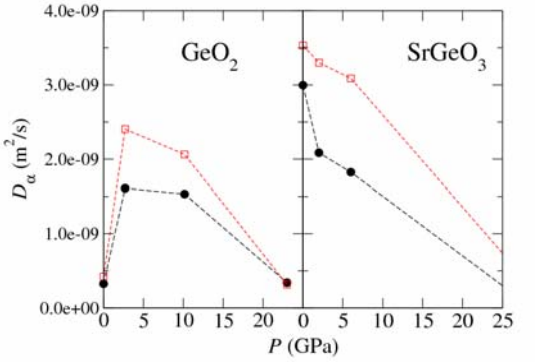

Fig. 4. Pressure dependence of the diffusion coefficients D_α for α = Ge (solid circles) and O (open squares) atoms.

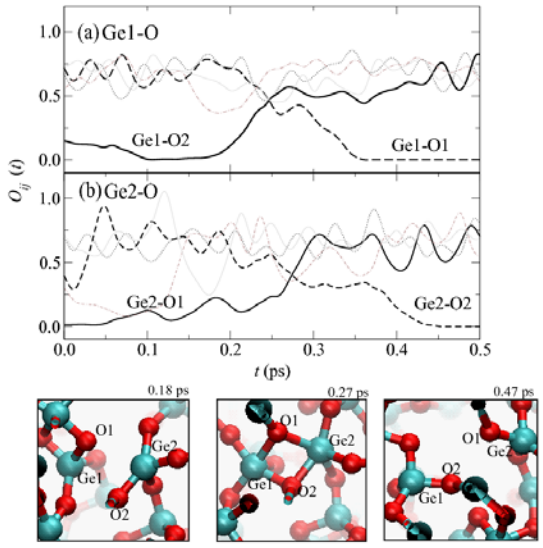

Fig. 5. (Top panel) The time evolution of bond-overlap populations $O_{ij}(t)$ for (a) i = Ge1, $j \in$ O and (b) i = Ge2, $j \in$ O in the process of the formation of a non-bridging oxygen. The thick sold and thick dashed lines show $O_{ij}(t)$ associated with the Ge and O atoms of interest as denoted in the figures. The thin lines show $O_{ij}(t)$ between the Ge atoms of interest (labeled as 'Ge1' and 'Ge2') and their neighboring O atoms except O1 and O2. (Bottom panel) Atomic configurations at t = 0.18, 0.27 and 0.47 ps. The large and small spheres show Ge and O atoms,

respectively.

Figure 5 shows this process at about 4 GPa. The concerted reactions with two over-coordinated Ge atoms can take place because Ge atoms are more easily coordinated to five O atoms under higher pressure. The important point is that non-bridging oxygen is not required in this mechanism while the formation of non-bridging oxygens are always involved in diffusion process at ambient pressure. Since liquid $SrGeO_3$ has non-bridging oxygens in normal condition, the formation of non-bridging oxygens isn't needed for atomic diffusion at ambient pressure. This is why the diffusivities of liquid $SrGeO_3$ are much higher than those of liquid GeO_2 which doesn't have non-bridging oxygens at ambient conditions. The diffusion mechanism of liquid $SrGeO_3$ doesn't change so much even when the pressure increases. Therefore, the diffusivities of liquid $SrGeO_3$ decrease monotonically with increasing pressure.

4 Summary

The microscopic mechanism of atomic diffusion in liquid GeO_2 and $SrGeO_3$ has been investigated by *ab initio* molecular-dynamics simulations. In liquid GeO_2, it has been found that the formation of non-bridging oxygen is always necessary for atomic diffusion at ambient pressure. When the pressure increases, the usual concerted reactions become possible. We have found that the atomic diffusion with concerted reaction gives the diffusion maximum under pressure. In liquid SrGeO3, on the other hand, the atomic diffusion without generating non-bridging oxygens is possible at ambient pressure. Even when the pressure increases, the diffusion mechanism of liquid $SrGeO_3$ doesn't change. Threrefore, liquid $SrGeO_3$ have no diffusion maximum under pressure.

Acknowledgments

The present work was supported by Grant-in-Aid for JSPS Fellows. The authors thank Research Institute for Information Technology, Kyushu University for the use of facilities. The computation was also carried out using the computer facilities at the Supercomputer Center, Institute for Solid State Physics, University of Tokyo.

References

1. S. K. Sharma, D. Virgo, and I. Kushiro, J. Non-Cryst. Solids **33**, 235 (1979)
2. K. Funakoshi, A. Suzuki, and H. Terasaki, J. Phys.: Condens. Matter **14**, 11343 (2002)
3. D. Marrocchelli, M. Salanne, and P. A. Madden, J. Phys.: Condens. Matter **22**, 152102 (2010)
4. B. B. Karki, D. Bhattarai and L. Stixrude, Phys. Rev. B **78**, 104205 (2007)
5. S. Ohmura and F. Shimojo, Phys. Rev. B **81**, 014208 (2010)
6. G. Gordon, S. Smith, and P. B. Isaacs, Acta. Cryst. **17**, 842 (1964)
7. Y. Shimizu, Y. Syono, and S. Akimoto, High Temp. High Press. **2**, 113 (1970)
8. P. E. Bl¨ochl, Phys. Rev. B **50**, 17953 (1994)
9. G. Kresse and D. Joubert, Phys. Rev. B **59**, 1758 (1999)
10. J. P. Perdew, K. Burke and M. Ernzerhof, Phys. Rev. Lett. **77,** 3865(1996)
11. G. Kresse and J. Hafner, Phys. Rev. B **49**, 14251 (1994)
12. F. Shimojo, R. K. Kalia, A. Nakano and P. Vashishta, Comp. Phys. Comm. **140**, 303 (2001)
13. S. Nos´e, Mol. Phys. **52**, 255 (1984)
14. W. G. Hoover, Phys. Rev. A **31**, 1695 (1985)
15. M. Tuckerman, B. J. Berne and G. J. Martyna, J. Chem. Phys. **97**, 1990 (1992)
16. P. B. Macedo, W. Capps, and T. A. Litovitz, J. Chem. Phys. **44**, 3357 (1966)
17. R. S. Mulliken, J. Chem. Phys. **23**, 1833 (1955), J. Chem. Phys. **23**, 1841 (1955)
18. F. Shimojo, A. Nakano, R. K. Kalia, and P. Vashishta, Phys. Rev. E **77**, 066103 (2008)